2020

Reservoir characterization and static Earth model for potential CO2 storage in Upper Pennsylvanian Cyclothems, Nebraska, USA

V.L. Smith

R.M. Joeckel
University of Nebraska - Lincoln

Reservoir characterization and static earth model for potential carbon dioxide storage in Upper Pennsylvanian cyclothems, Nebraska, United States

Valerie L. Smith and R. M. Joeckel

ABSTRACT

This study estimates the carbon storage potential of interbedded shales and carbonate rocks (cyclothems) in the Pennsylvanian Lansing and Kansas City groups (LKC) on the Cambridge arch in southwestern Nebraska. This effort is essential to the development of a CO_2 storage strategy for the Integrated Midcontinent Stacked Carbon Storage Hub project as part of the Department of Energy–National Energy Technology Laboratory's Carbon Storage Assurance Facility Enterprise initiative. We present a static earth (SE) model representing the 250-ft (76-m)-thick LKCs. This model is based on vintage (mostly pre-1970) well logs from the Sleepy Hollow field (Red Willow County, Nebraska) as well as a new (June 2019) stratigraphic test well drilled expressly for the purpose of the present study. Interpretations of advanced petrophysical logs and cores from this new well were crucial ingredients in the development of the geologic framework for SE model development. Gamma-ray (GR) logs readily differentiate carbonate and mudstone units within the LKC, allowing the differentiation of three GR facies for use in a facies model. Carbonate rock units, which are composed of multiple textures, were correlated across the field. We capture the heterogeneity of these carbonates during petrophysical modeling using effective porosity logs along with Gaussian random function simulation conditioned by the three-dimensional facies model. The SE model was used in computing carbon storage estimates for each LKC carbonate zone over an area of 1 mi^2. In total, supercritical CO_2 storage is estimated at 602,157 t/mi^2 (232,494 t/km^2) when using a deterministic saline storage efficiency factor of 0.1.

Manuscript received August 1, 2019; provisional acceptance January 22, 2020; revised manuscript received February 24, 2020; final acceptance February 28, 2020.

DOI:10.1306/eg.01222019018

AUTHORS

Valerie L. Smith ~ *Department of Critical Infrastructure, Battelle, Columbus, Ohio; SmithVL@battelle.org*

Valerie L. Smith has served as a reservoir geophysicist with Battelle and Schlumberger. A keen user of Petrel's integrated geomodeling workflows since 2008, she has supported more than 20 CO_2 geologic storage projects in the United States and Canada. Her experience includes site assessment, subsurface interpretation, reservoir characterization, microseismic monitoring, and three-dimensional geocellular modeling. She holds degrees in engineering science, physics, and geology. She is the corresponding author of this paper.

R. M. Joeckel ~ *Conservation and Survey Division, Department of Earth and Atmospheric Sciences, School of Natural Resources and State Museum, University of Nebraska–Lincoln, Lincoln, Nebraska; rjoeckel3@unl.edu*

R. M. Joeckel is the state geologist of Nebraska and director of the Conservation and Survey Division, School of Natural Resources, University of Nebraska–Lincoln. His research interests include stratigraphy and sedimentology, paleosols, fluvial systems, and sedimentary geochemistry. He holds a Ph.D. in geology from the University of Iowa.

ACKNOWLEDGMENT

The Integrated Midcontinent Stacked Carbon Storage Hub project is supported by the US Department of Energy–National Energy Technology Laboratory Agreement no. DE-FE0029264 and DE-FOA-0031623.

INTRODUCTION

The Integrated Midcontinent Stacked Carbon Storage (IMSCS) hub project is part of the Department of Energy–National Energy Technology Laboratory's Carbon Storage Assurance Facility Enterprise initiative. This project seeks to develop a regional carbon storage hub or corridor connecting sources of captured carbon to existing oil fields for carbon storage and enhanced oil recovery (EOR). This research supports the assessment of geologic CO_2 storage for sites in Nebraska and Kansas. The project began with the analysis of a study area in southwestern Nebraska centered on Sleepy Hollow field (SHF) (Figure 1). This site was selected because the potential reservoir units and seals in the Pennsylvanian Lansing and Kansas City groups (LKC) were determined to be of sufficient depth and quality for CO_2 storage. The LKC is dominated by limestones and mudstones, and it has long been interpreted as a succession of "Kansas-type" cyclothems (e.g., Heckel, 1986, 1991). Our analyses of trends in gamma-ray (GR) and neutron-porosity (NPHI) logs as well as new data generated in the course of this study reinforce the longstanding hypothesis that the LKC was deposited under conditions of fluctuating eustatic sea level (Heckel, 1986).

Although the common CO_2 storage concept is composed of a distinctive reservoir and seal pair, the storage assessment for the LKC is complicated by the stacking of reservoirs and seals, some of which are hydrocarbon-bearing. A successful storage strategy for the LKC depends on a detailed understanding of the development and occurrence of porosity in carbonate strata.

Reservoir characterization began with the compilation of vintage (mostly pre-1970s) well logs from the study area. Existing subsurface interpretations of the LKC (Watney, 1980; Dubois, 1985) from nearby oil fields were also incorporated in the characterization of potential storage units. Subsurface interpretation and reservoir characterization provided the basis for a static earth (SE) model representing the LKC. Existing core samples from Sleepy Hollow and neighboring oil fields show that porosity exists primarily in packstone and grainstone units.

Observations from cores and logs demonstrate that LKC strata can be subdivided into limestone-dominated, mudstone-dominated, and shale-dominated packages of strata. The GR log thresholds, which represent important differences in reservoir (or seal) quality, were used to quantitatively define these three packages of strata as GR facies. The NPHI logs were used during the three-dimensional (3-D) petrophysical property modeling; however, they were a poor indicator of effective porosity because of the clay-bound water that is commonly present within mudstones. The NPHI log responses to clay-bound water complicated the derivation of effective porosity logs and, therefore, posed a substantive problem in this project. This problem was resolved through comparative analysis using core samples.

GEOLOGIC SETTING

Red Willow County (Figure 1A) has numerous oil fields originating in the early 1960s (Busch, 1977). Maps of formation tops in these oil fields show the Cambridge arch (Moore and Nelson, 1974) as a northwesterly continuation of the Central Kansas uplift. Together, this structural uplift trends from the northwest to the southeast (see Figure 1A). The primary study area for this storage project, SHF, is a very gentle anticline located on the southwestern part of the Cambridge arch, and it contains more than 200 wells, many of which barely penetrated weathered basement rocks (Figure 1B). Oil production for SHF has been from the LKC stratigraphic zone C as well as from a thin sandstone that directly overlies the basement rock (Rogers, 1977) (Figure 2). This basal sandstone is locally referred to as the "Sleepy Hollow sandstone," and it is also labeled as the oil-producing "Reagan unit" in some logs. It remains unclear, however, whether this sandstone is indeed equivalent to, and of the same age as, the regionally extensive Reagan sandstone (Cambrian), or whether it is a localized, basal Pennsylvanian deposit.

The preliminary target reservoirs for CO_2 sequestration are stacked carbonate rocks in the Pennsylvanian System, which are the same limestone strata that may produce petroleum (see Figure 2). The aforementioned basal sandstone is also considered a potential reservoir for carbon storage. The Pennsylvanian System is dominated by cyclic packages of carbonates and mudrocks, the origins of which are attributed to glacioeustatic sea-level fluctuations in shallow seas on an epicontinental platform. The characterization of these carbonates and their representation in an SE model is the central theme of this paper. Cap-rock intervals in the study area are also cyclically stacked and consist of a series of tighter, mudstone units that separate the comparatively porous carbonate intervals. The deeper, basal sand unit is also overlain by mudstones in the Pleasanton and Marmaton

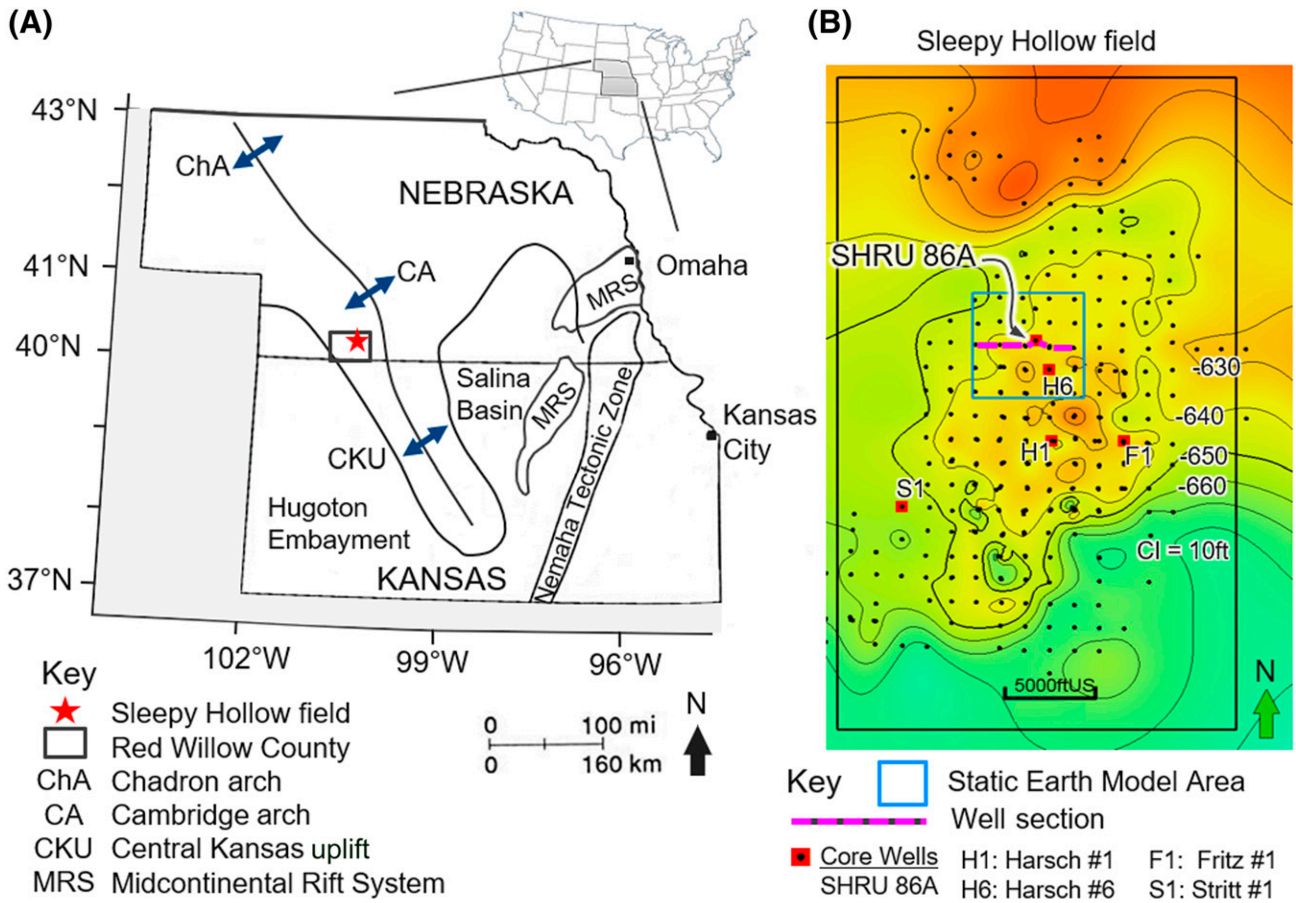

Figure 1. (A) Location of Sleepy Hollow field (SHF) on the southwestward limb of the Cambridge arch in Nebraska. (B) The SHF study area outlined by black rectangle. Well coverage is shown as black dots. Red boxes represent wells with core samples. Pink line represents well section. Blue box represents footprint of static earth model reported in this paper. Contours are elevation depth (feet, mean sea level) for the top of the Pennsylvanian Lansing and Kansas City groups. CI = contour interval; SHRU 86A = Sleepy Hollow Reagan unit 86A.

groups underlying the LKC (Figure 2). The basic well-log suite for many of the wells in the SHF (Figure 1B) includes GR, NPHI, and resistivity (R) logs; there are cored intervals in a very few of these wells.

An example of the carbonates' apparent cyclicity is shown in Figure 3 from wells central to the SHF that were drilled to approximately 3520 ft (~1073 m). The total depth of the new Sleepy Hollow Reagan unit (SHRU) 86A well is 3636 ft (1108 m). At an approximate depth of 3150 ft (~960 m) and thickness of 250 ft (76.2 m), the LKC has been subdivided by well drillers into the lettered stratigraphic zones (A–F) in southwestern Nebraska. However, conventions for lettering LKC stratigraphic zones are different in Nebraska and Kansas, potentially adding an element of confusion to the interpretation of the succession. Lettered stratigraphic zones in the LKC range from 28 to 64 ft in thickness (8.5 to 19.5 m). Each zone is composed of carbonates (oolitic, peloidal, and skeletal grainstones, plus other, less porous textures) and mudrocks (mudstones and shales). Some of these lithologies are tight; therefore, each carbonate zone has storage restrictions determined by the magnitude and stratigraphic distribution of porosity. The top of weathered basement rock is penetrated at approximately 3550 ft (~1082 m) measured depth (see Figure 3). The interpreted base of the LKC (commonly labeled the "Kansas City Base") is also the undifferentiated top of either the Pleasanton or Marmaton Groups.

The gentle geologic structure in the SHF has been determined primarily by mapping formation tops in the absence of seismic surveys. Structural mapping of formation tops, such as the top of the LKC, reveals a gentle anticlinal structure in the study area (see Figure 1B). Although the LKC is considered the primary storage section, a thin sandstone at the base of Phanerozoic

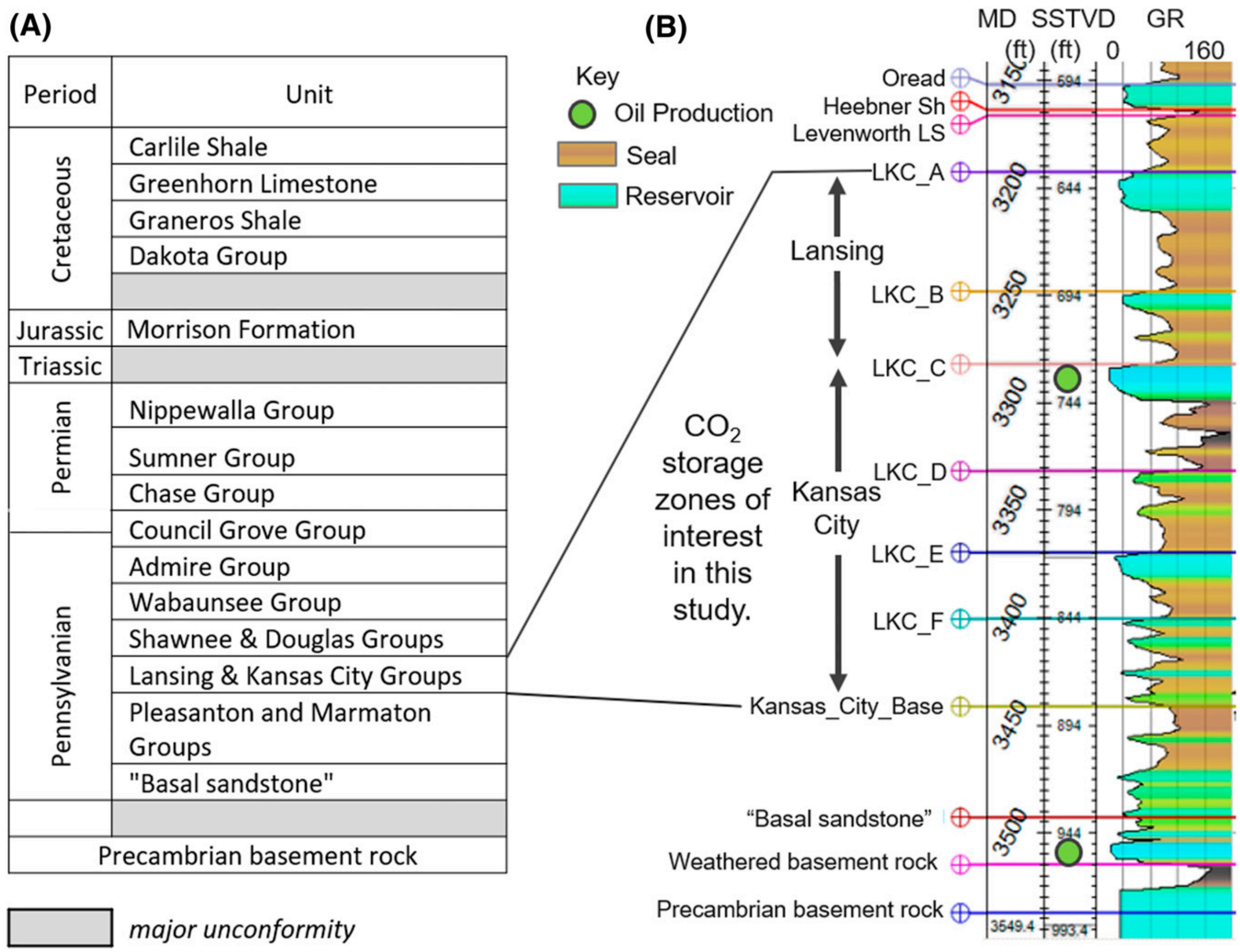

Figure 2. (A) Simplified stratigraphic column showing the deep saline formations of interest and overlying cap rocks evaluated in the Cambridge arch study area. (B) Example of gamma-ray (GR) log response for the Pennsylvanian Lansing and Kansas City groups (LKC) where members are commonly lettered A through F. LS = Limestone; MD = measured depth; Sh = Shale; SSTVD = subsea true vertical depth.

sedimentary-rock cover (Sleepy Hollow sandstone or the putative Reagan unit) has also been studied for storage capacity. This sandstone is believed to pinch out eastward against the Cambridge arch (Rogers, 1977). On the basis of well penetrations, we surmise that local, gentle basement topography controls the distribution of this thin sandstone in the study area. We have no evidence that this basement topography is directly associated with any geologic structures smaller than the scale of the Cambridge arch itself. The SHRU 86A well penetrated no faults. The sedimentary succession penetrated by the borehole contained two open fractures, although the weathered (~22 ft thick) and intact basement-rock (~87 ft thick) intervals in the borehole contained many open fractures. We also note that 50 microseismic events in Phanerozoic sedimentary cover and 126 microseismic events in basement rock were documented around the study area during a short-term monitoring program in the 1980s (Evans and Steeples, 1987). Nevertheless, the relationships between these microseismic events and any hypothetical geologic structures, or between them and water injection EOR, remains unclear more than three decades later.

Establishing a Stratigraphic Framework for the Static Earth Model

We interpret the stratigraphic framework for the LKC in the context of the existing model for Pennsylvanian cyclothems in Midcontinent, United States. The Kansas-type cyclothem (e.g., Heckel, 1986; Heckel and Watney, 2002) (Figure 4A) proposed in studies of the Pennsylvanian outcrop belt, far to the east of our study area, is bounded below by an "outside" shale (in fact,

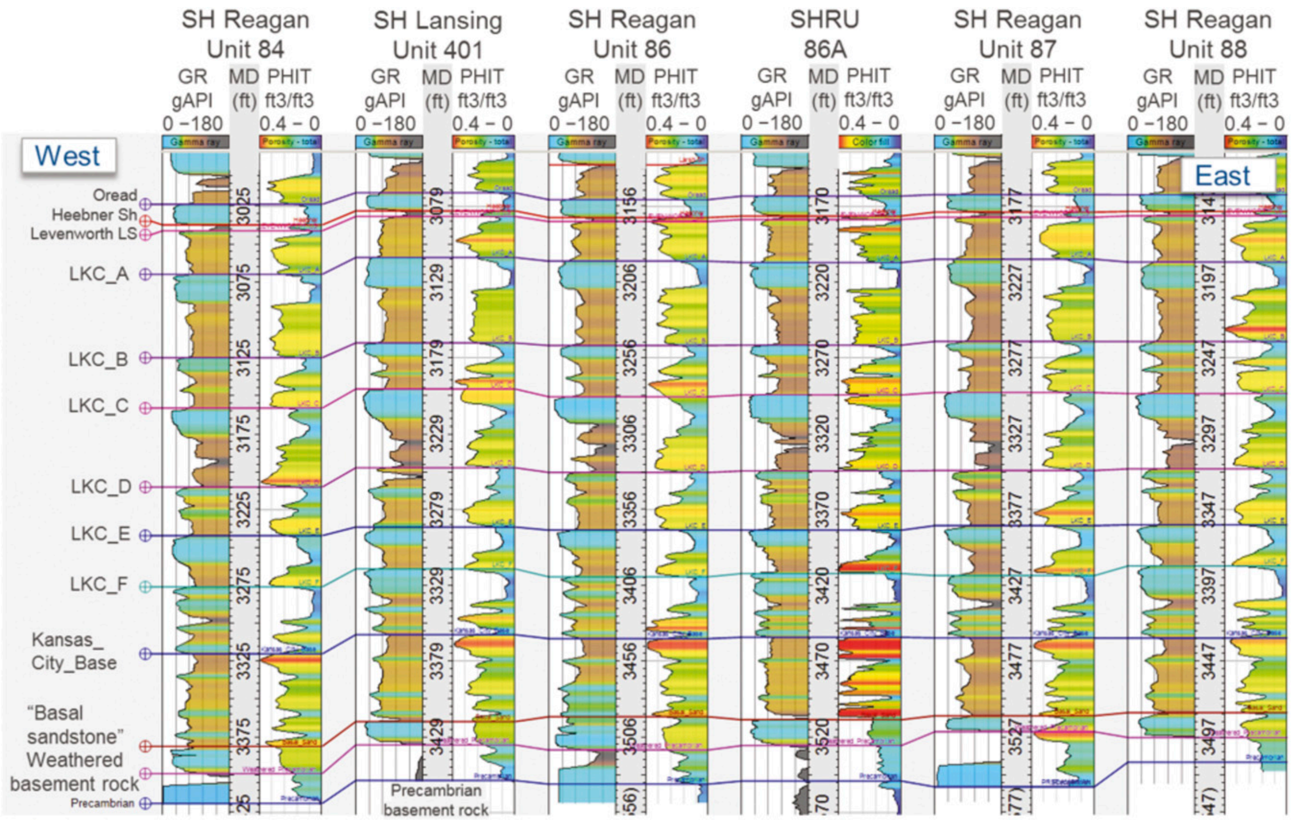

Figure 3. Gamma-ray (GR) and total porosity logs (PHIT) for six wells fully penetrating the Lansing and Kansas City groups (LKC) section. The repetitive patterns in these logs are compatible with the putative cyclicity of carbonates and mudrocks in the succession. The LKC zones are picked on top of key carbonate units. See Figure 1B for well-section location. LKC_A–LKC_F = zones within the Pennsylvania Lansing and Kansas City groups; LS = Limestone; MD = measured depth; SH = Sleepy Hollow; SHRU 86A = Sleepy Hollow Reagan unit 86A.

typically in part, or in its entirety, massive mudstone or claystone) that exhibits evidence for subaerial exposure and soil development. A comparatively thin transgressive limestone exists atop the outside shale, and the transgressive limestone is overlain by a deeper-water "core" shale. Atop the core shale is a thick regressive limestone that is overlain by another outside shale (Figure 4A). Black core shales are typified by significant peaks in the GR log response.

Salient challenges exist in applying the outcrop-based cyclothem model to our study area, which is far to the west on a structural high in the subsurface. Chiefly, evidence for the black core shales is markedly less in the study area than in other parts of the midcontinent Pennsylvanian platform. Although some darker shale units are present in particular stratigraphic positions that are comparable to those of core shales in the outcrop belt, GR logs indicate that such instances are not the rule (see Figure 3). Thus, where such shales are missing, transgressive limestone units are directly overlain by regressive limestones (Figure 4B), effecting the appearance of a single, very thick limestone package in GR logs (Figure 4C). The LKC zone B, which is composed of two cyclothems, is a notable example (Figure 5). The transgressive core shales in the equivalent outcropping interval, the Eudora and Hickory Creek shale members, appear to be absent or, at least, there are no GR peaks corresponding to them in the present study area (see Figure 5). In comparison, the Diopita A-16 well, 82 mi southeast of the present study area, shows more instances of black core shales, both in GR logs and core (Young, 2011). We surmise that local paleogeography and environmental conditions (bathymetry, circulation, availability of sediment and organic matter, etc.) on and around the Cambridge arch, even in the context of eustatic sea-level changes, were unsuitable for the deposition of typical core shale facies. Accordingly, we present a revised sea-level curve (see Figure 4B) for the study area.

Interpretation of Cores and Thin Sections

Detailed descriptions of a few preexisting cores in the study area and a small but representative set of thin

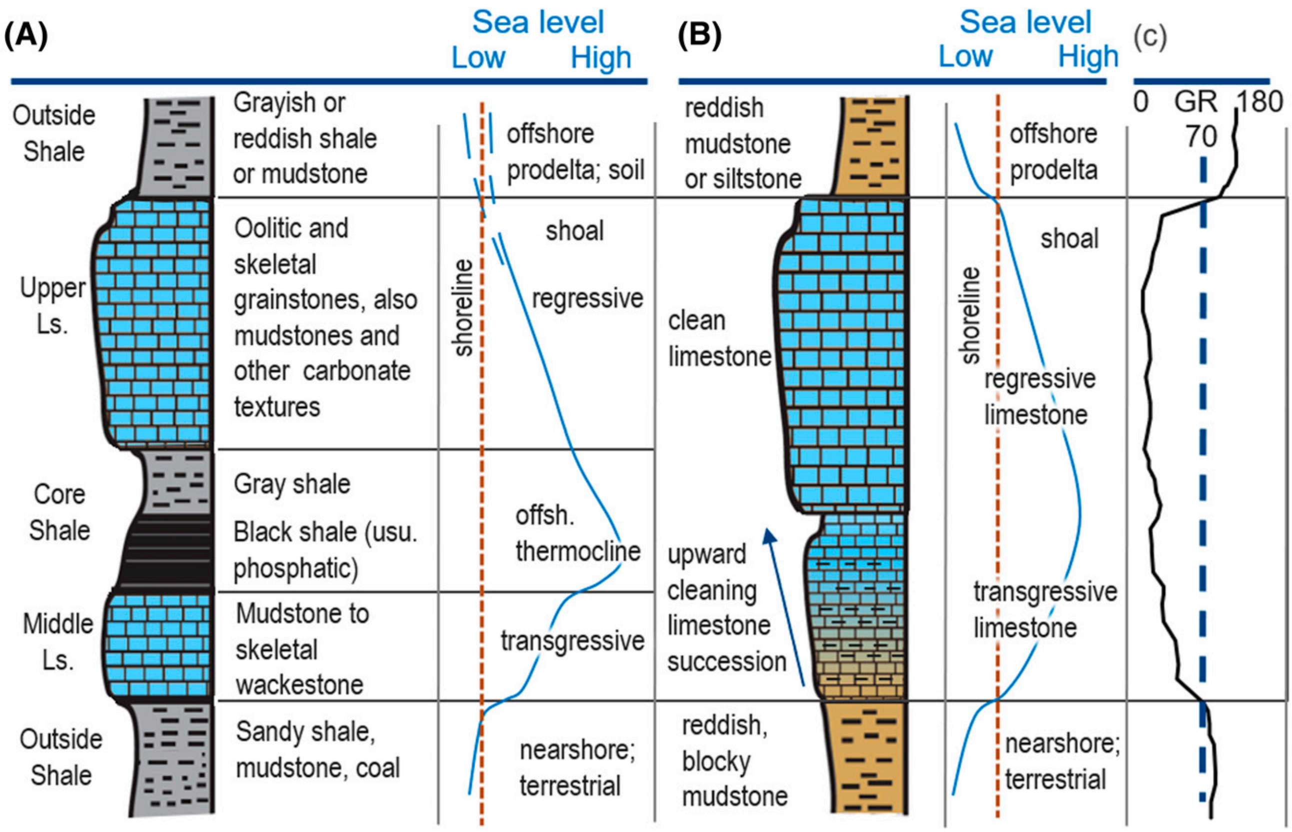

Figure 4. Pennsylvanian carbonate cycle. (A) Example of Kansas-type cyclothem, modified after Heckel (1986). (B) Adaptation of the carbonate cycle more commonly seen at Sleepy Hollow field, Nebraska. (C) Representative gamma-ray (GR) log response usually seen for carbonate units like that shown in (B). Ls. = Limestone; offsh. = offshore; usu. = usually.

sections produced from those cores were the basis for a characterization of critical lithologies (carbonate rocks and mudstones) in the LKC.

Example sidewall core samples from the LKC are described in Table 1 and are plotted, in depth, against GR log response for the SHRU 86A well (Figure 6). These sidewall cores correlate with the GR logs, with low GR response corresponding to carbonate rock and higher GR reflecting clay-rich mudstones. Although discrimination of carbonate textures cannot be determined based on wire-line logs, the GR log is sufficient as a standalone input for development of a coarse facies model.

Several outcrop- and core-based studies of the LKC across Kansas and in Nebraska have demonstrated not only that mudstones and wackestones are common limestone textures in the LKC but also that grainier limestone facies appear at particular stratigraphic levels (Heckel, 1986, 1994, 2008). Oolitic, skeletal, and peloidal grainstones in the LKC were targeted for the assessment of CO_2 storage in the SHF and sampled for petrography and mineralogy. In the Harsch #6 well, oolitic grainstones exhibit dominantly moldic and vugular porosity and very minor intergranular porosity (Figure 6F; H1 in Figure 1B). Individual ooids are uniformly recrystallized to calcite microspar. Peloidal and skeletal grainstones were also encountered (Figure 6G). The peloids in such rocks are mictitic overall but also partially neomorphosed, and they have indistinct or very indistinct outlines. Peloid-dominated domains exhibit both intergranular and intragranular porosity. Skeletal allochems in grainstone domains include fusulinids and ostracodes, fragments of brachiopods and bryozoans, and undetermined fossil fragments. In some thin sections, most of the skeletal grains have micritized envelopes (Figure 6E). Some larger skeletal allochems (e.g., brachiopod fragments) have also been replaced by coarse, blocky calcite spar. Rare open voids that appear to be molds of large skeletal allochems may indeed represent very minor moldic porosity, or they may be the results of the plucking of void filling spar during thin-section preparation. Only one limestone sample proved to be partially dolomitized, but because so few thin sections were produced, the overall incidence of dolomitization cannot be determined.

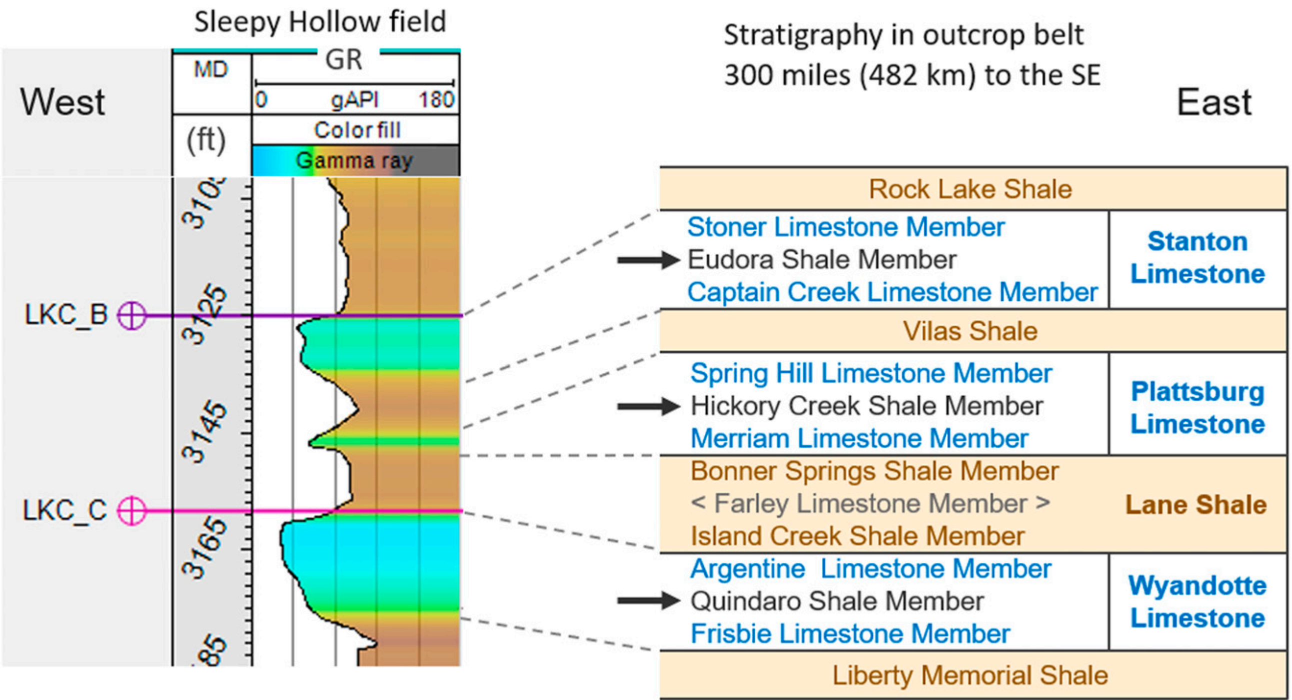

Figure 5. Interpretation of Pennsylvanian carbonate cycles at Sleepy Hollow field and their correlative geologic member names as formally named in outcrops, using the revised stratigraphic scheme Heckel and Watney (2002). The intervening transgressive shale units (marked by arrows) are either absent or too thin to be resolved by gamma-ray (GR) logging. The thicker regressive shale units tend to be mudstones and have pedogenic features. LKC = Pennsylvanian Lansing and Kansas City groups; LKC_B–LKC_C = two zones within the LKC; MD = measured depth.

Mudstones are the only truly widespread clastic rocks in the LKC overall. The lithologic characteristics of lamination and fissility that were criteria for identifying clay and silty clay shales in the direct examination of core samples are supported by the identification of 0.5–3.0-mm laminae in thin sections of the same materials (Figure 6H). Likewise, claystones that were characterized as being massive during the description of cores exhibited no well-organized depositional sedimentary structures in thin sections and, instead, exhibited small granular to blocky aggregates that probably represent preserved soil structure (Figure 6I). Birefringence fabrics in our comparatively few thin sections of mudstones are mostly masked by abundant iron oxides that impregnate rock matrices, making it very difficult to differentiate patterns of optical anisotropy that might be of primary depositional origins to those that may have been produced by subsequent pedogenesis. Representative thin sections and their descriptions are summarized in Table 2 and shown against a GR log (see Figure 6).

Many of the mudstones that we examined closely in our study are at least partially reddened because either (1) the precursor sediments were already oxidized when they were deposited or (2) the oxidation of these sediments occurred after deposition and in association with an overlying subaerial exposure surface. Several paleosols have been documented in mudstones within the LKC and other Upper Pennsylvanian cyclothems both in the outcrop belt and in the deep subsurface far to the west (Prather, 1985; Joeckel, 1989, 1994, 1999).

Interpretation of Log Data

We characterize the SHF using vintage (mostly pre-1970) well logs from 205 wells located predominately

Table 1. Example Sidewall Core Samples from Sleepy Hollow Reagan Unit 86A

ID*	Description
(a)	Limestone. White, with stylolite, appears tight, some dolomite near stylolite.
(b)	Mudrock. Dark grayish green, laminated, more shaley.
(c)	Limestone. Oil stained in parts, pinpoint vugs, possible moldic porosity, greyish-white.
(d)	Mudrock. Reddish, muddy, clay, unconsolidated.

*ID = identification (corresponds to samples shown with gamma-ray well log in Figure 6).

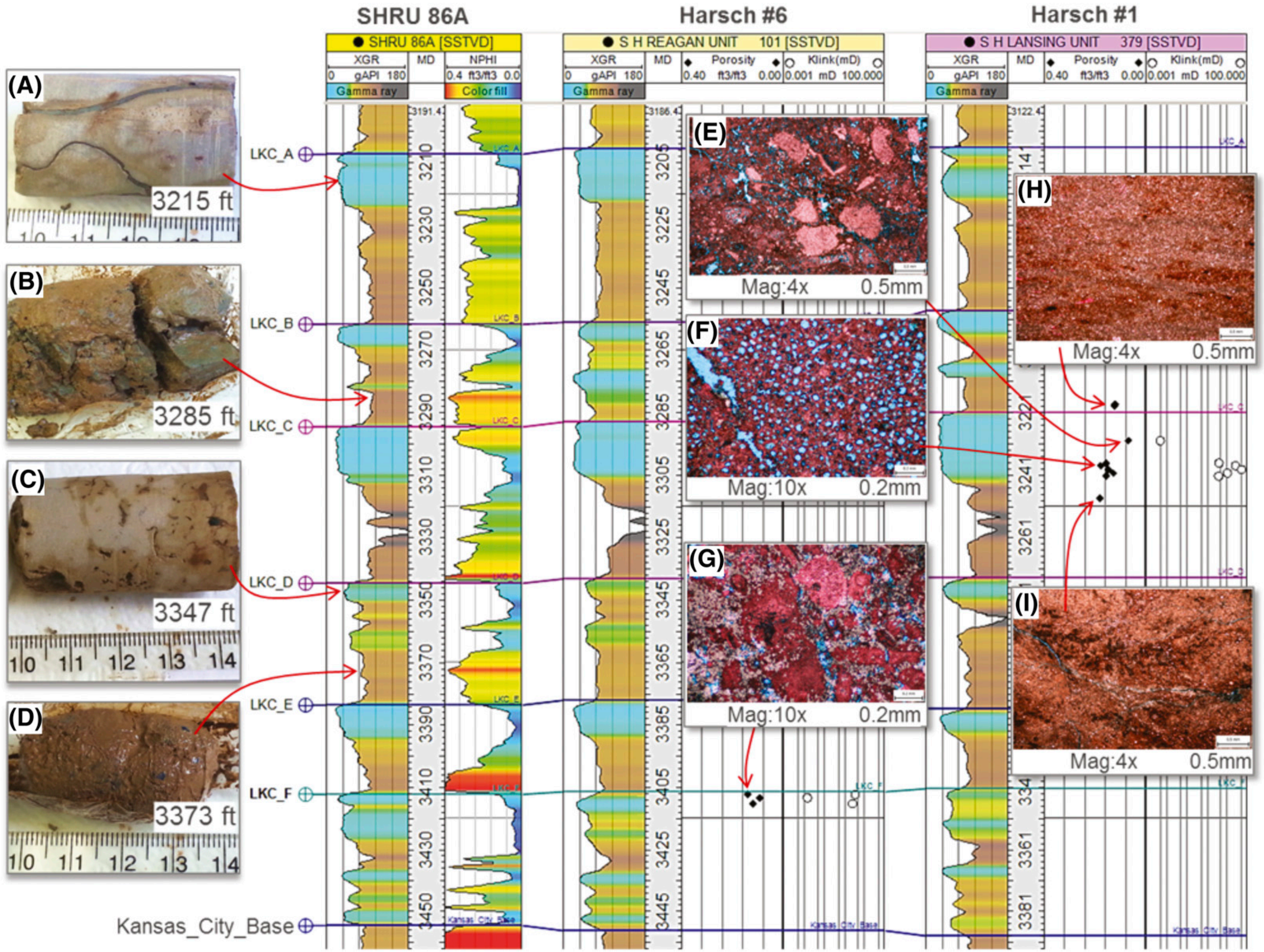

Figure 6. Representative sidewall core samples and thin sections with gamma-ray logs. (A) Limestone. (B) Mudrock. (C) Limestone. (D) Mudrock. (E) Grainstone. (F) Oolitic grainstone. (G) Peloidal and skeletal grainstone. (H) Clay shale. (I) Claystone. Samples (A) through (I) are described further in Tables 1 and 2. Well locations are provided in Figure 1B. Klink = permeability, Klinkenberg test; LKC = Pennsylvanian Lansing and Kansas City groups; LKC_A–LKC_F = zones within the Pennsylvania Lansing and Kansas City groups; MD = measured depth; NPHI = neutron porosity; SHRU 86A = Sleepy Hollow Reagan unit 86A; SSTVD = subsea true vertical depth; XGR = gamma-ray log.

Table 2. Example Pennsylvanian Lansing and Kansas City Groups Thin-Section Descriptions

ID*	Lithology	Description	Porosity and Permeability
(e)	Grainstone	Partially micritized skeletal grains with micrite envelopes, fusulinids, fragments of coralline red algae. Dominantly intergranular porosity and subordinate intragranular porosity	Phi = 6.94% K = 0.017 md
(f)	Oolitic grainstone	Ooids have been recrystallized to microspar. Dominantly moldic and vugular porosity; very minor intergranular porosity	Phi = 17.86% K = 33.962 md
(g)	Peloidal and skeletal grainstone	Recrystallized and partially dolomitized. Largely recrystallized calcitic allochems (echinoderms, brachiopods, ostracodes, and indeterminate), many of which have micrite envelopes. Peloids with indistinct to very indistinct outlines, partially to mostly dolomitized microspar, and finely crystalline dolomite	Phi = 14.11% K = 3.942 md
(h)	Clay shale	Silt at 10× magnification. Laminae 0.4–1.2 mm thick, indeterminate (few calcitic, invertebrate skeletal grains). Few opaque iron oxide mottles roughly parallel to lamination. The XRF result for hematite: 3.29%	Phi = 12.30% K = 0.001 md
(i)	Claystone	Silt at 10× magnification. Massive; possible soil structure (very fine-fine, granular), silt-filled crack infillings or burrows approximately 0.2–1.0 mm in width weak speckled birefringence fabric; partial masking of birefringence by iron oxides; drab mottling. Porosity appears to be entirely the result of fracturing after collection, preparation, and plucking. The XRF result for hematite: 5.28%	Phi = 18.05% K = 0.001 md

Abbreviations: K = permeability; XRF = x-ray fluorescence.
*ID = identification (corresponds to samples shown with gamma-ray well log in Figure 6).

within the field and several from outside the field. These well logs typically include GR, NPHI, spontaneous potential, and R. Core interpretations and thin sections are based on five wells in and around SHF and include LKC zones B, C, and F (see Figure 1B).

Data obtained from the new SHRU 86A stratigraphic test well included the logs mentioned above plus a full suite of advanced logs including a fullbore formation microimager (FMI) borehole image log, nuclear magnetic resonance (NMR) logging, and elemental capture spectroscopy (ECS) logging. These new logs have provided further validation of our preliminary differentiations of limestones and mudstones.

The static FMI log shows very sharp upper contacts for the regressive limestones that are overlain by mudstones and can be used to refine our LKC zonal picks (Figure 7). Darker areas in the image are caused by conductive intervals attributed to clay-bound water in the mudstones. Although conductive and porous, laboratory-measured results in Table 2 show that the mudstones are indeed tight with a permeability of 0.001 md. In contrast, the light areas on the FMI log correspond to the resistive carbonate units, which would suggest lower porosity. The porosity of the carbonate rocks varies significantly, but more importantly, these rocks do have some permeability (Table 2).

The goal of the NMR logging in SHRU 86A was to accurately identify clay-bound water so that it could be eliminated from total porosity, thereby producing more reliable estimates of effective porosity. Unfortunately, the NMR log response proved very sensitive to the thick mud cake that accumulated on the particularly rugose

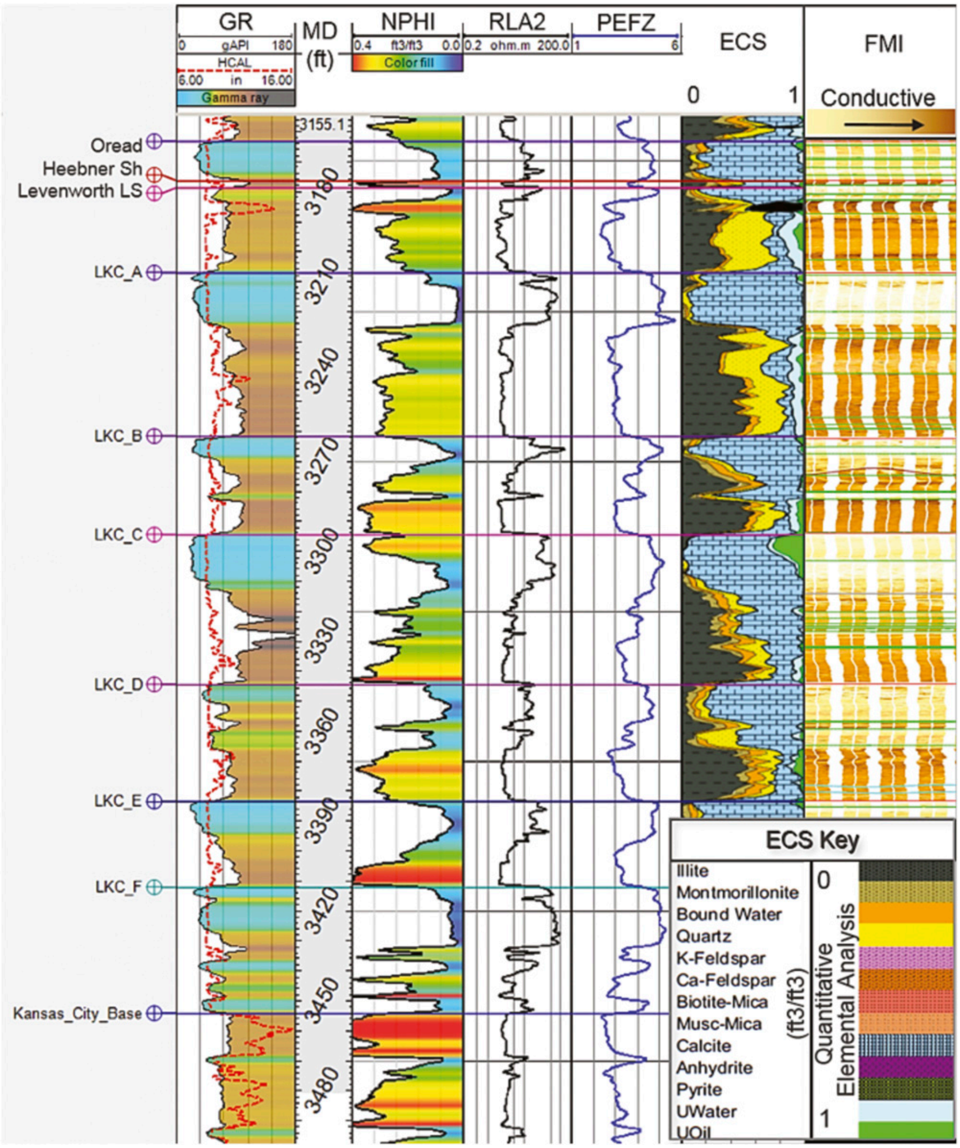

Figure 7. Logs from stratigraphic test well Sleepy Hollow Reagan unit 86A showing Pennsylvanian Lansing and Kansas City groups (LKC) zones A through F. ECS = elemental capture spectroscopy; FMI = fullbore formation microimager; GR = gamma ray; HCAL = caliper; LKC_A–LKC_F = zones within the Pennsylvania Lansing and Kansas City groups; LS = Limestone; MD = measured depth; Musc = muscovite; NPHI = neutron porosity; PEFZ = photoelectric factor; RLA2 = resistivity; Sh = Shale; UOil = movable oil; Uwater = movable water.

mudstone sections of the borehole wall. Therefore, the NMR logging tool could not sense deeply and predict free fluid volumes (effective porosities) in limestone reservoirs. The ECS tool, however, penetrated deeper and its results are considered reliable, especially in the context of GR and NPHI logs and the examination of core samples.

The ECS logging in the SHRU 86A well provides an additional check on the assignment of GR facies. To wit, it verifies the dominance of calcite in our limestones (our carbonate-dominated GR facies) and the dominance of clay minerals and quartz in shales and mudstones (see Figure 7). This information coupled with observations we have made from core and thin sections provide a better integrated picture for LKC intervals where core is absent.

STATIC EARTH MODEL DEVELOPMENT

The carbon storage assessment for SHF required the development of an SE model representing the petrophysical properties of the reservoir units and cap rocks. Hydrologically, the LKC is an open system in which the storage area and thickness are relatively well defined by well control. The modeling workflow steps are described in what follows and conclude with CO_2 storage estimate calculations.

The geomodeling workflow is summarized in Figure 8.

Data Acquisition

Well logs from approximately 205 wells in and around SHF were collected and digitized (Bacon et al., 2018). Well top picks and well header data were compiled. Existing core samples in the study area were identified and submitted for core analysis. A new well, SHRU 86A, was drilled, cored, and logged in June 2019.

Data Quality Control

Well-log data went through an extensive quality control process that included the validation of wellhead elevations and formation-top picks. The GR logs were normalized to ensure that the range of their response was similar among the 200+ wells. The NPHI logs were

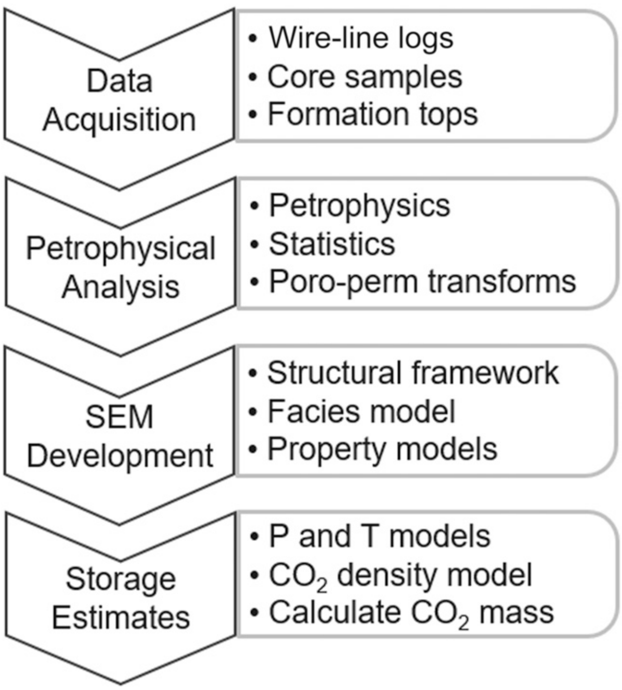

Figure 8. Workflow for the construction of geocellular models to calculate the effective storage resource potential for CO_2. Poro-perm = porosity–permeability; P = pressure; SEM = static earth model; T = temperature.

sensitive to the clay-bound water porosity and so it was necessary to prepare effective porosity logs. The shale volume (V-shale) correction method was used per equations 1 and 2:

$$V_{shale} = \left(GR_{log} - GR_{res}\right) \,/\, \left(GR_{shale} - GR_{res}\right) \quad (1)$$

where

V_{shale} = shale fraction (i.e., nonreservoir)
GR_{log} = GR log value
GR_{res} = GR value of clean (i.e., low clay) carbonate rock in each zone
GR_{shale} = GR value from a nearby shale interval

$$PHIe = PHI_t \times (1 - V_{shale}) \quad (2)$$

where

PHI_e = effective porosity
PHI_t = total porosity (uncorrected, typically NPHI)
$1-V_{shale}$ = sandstone fraction or carbonate fraction or both (i.e., reservoir fraction)

Data Import

Log data and available well tops were imported into a subsurface interpretation and modeling software that enabled the development of a 3-D geocellular, petrophysical model. The modeling package permits the computation of pore volume and the subsequent reporting of pore volume results by facies and by model zone.

Generate Surfaces and Static Earth Model Framework

Formation tops for the LKC were picked on the tops of low GR signatures (see Figures 3, 9A). These picks are consistent with the tops of regressive carbonates, which typically include the best reservoir-quality rock. This step provided an opportunity to pick missing formation tops and validate existing ones through well correlations in cross-section views. The high density of wells, their correlation, and the picking of tops provided the key input for creating surfaces.

Surfaces for many carbonate tops were created with the top picks using a convergent gridding algorithm. Surfaces for the LKC section down to basement were made across the SHF. The SE model framework presented here was constrained to 26 wells and represents a smaller part of the full field-scale SE model (Figure 10A). Surfaces were then used to define zones in the 3-D geocellular grid of the SE model (Figure 10B). Each zone was easy to correlate among wells across the field. The upper part of each zone was typically represented by a dominate limestone unit; some zones had two or more thinner limestones. The SE model grid is composed of cells that are 50 ft × 50 ft (15.4 m × 15.4 m). Each zone was then layered in 2-ft (0.61-m) increments, resulting in an SE model with 3,499,200 total cells (120i × 120j × 243k).

Facies Model

Facies models enable better control for delineating where and how petrophysical properties are distributed within each SE model zone. Within the LKC, individual lithostratigraphic units are laterally extensive and the greatest variability in rock characteristics is in the vertical direction. The GR log signatures provided the basis for dividing the zones into three lithofacies or flow units.

Stratigraphic intervals exhibiting low GR values (<70 gAPI) were attributed to clean limestones. These limestones may be mostly wackestones and mudstones; however, oolitic limestone and skeletal and peloidal grainstones are also present, and these textures have the best porosity. Units identified as limestones had better reservoir properties overall than the units that were identified as mudstones. Other studies (Watney, 1980; Young, 2011) have demonstrated that the clean, regressive limestones, especially those that were subjected to subaerial exposure prior to deep burial, have better porosity development.

Stratigraphic intervals exhibiting higher GR values (>70 gAPI) generally represent mudrocks. Mudrocks are considered to be low-permeability baffles that inhibit the vertical migration of CO_2. Thus, such units were considered as tight for modeling purposes. Putatively deeper-water, transgressive, offshore-marine shales (the black core shales of Heckel, 1986, 1994, 2008), which do not exist in all the cyclothems at SHF, produced very high GR responses (>120 gAPI). These shales are assumed to be tight in our GR facies determination, and they are combined with what we interpret to be regressive mudstones. We developed a simplified model consisting of three GR facies corresponding to general ranges of rock characteristics associated with GR responses (Figure 11; Table 3).

Our facies model was prepared in two steps: (1) using an arithmetic sampling method, the GR logs were sampled into the 3-D geocellular grid along their well trajectories. (2) These data were then interpolated into a 3-D grid using the moving average method with a point weighting of inverse distance squared. This deterministic approach can quickly populate the 3-D grid and can only

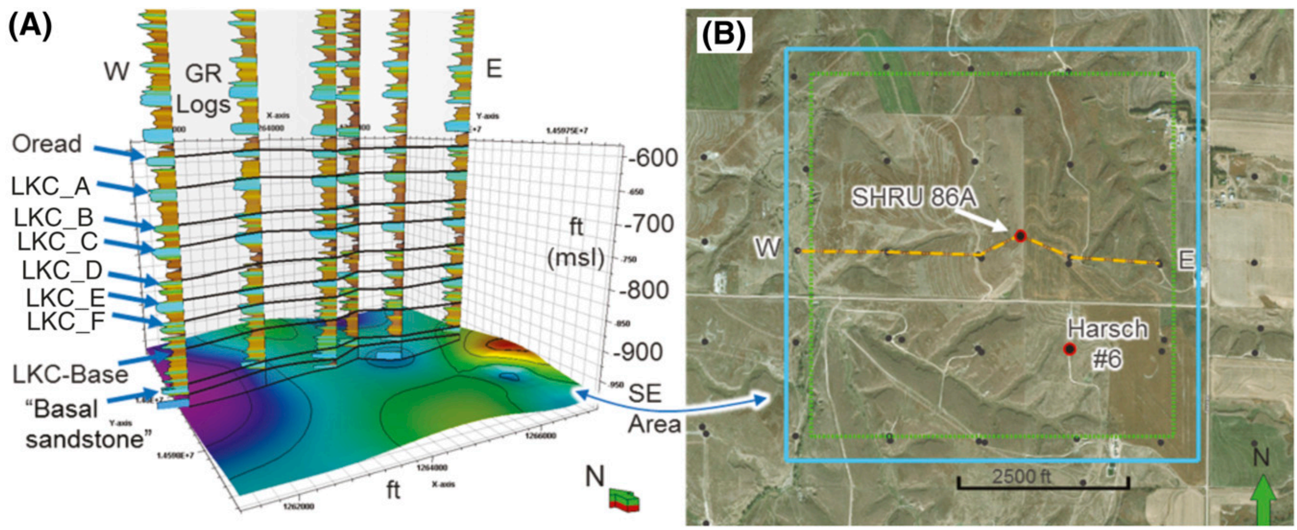

Figure 9. Well section across static earth (SE) model. (A) Well section showing Pennsylvanian Lansing and Kansas City groups (LKC) carbonate rock top picks based on gamma-ray (GR) logs. (B) Map view of SE model area and location of well section at left. Also shown are well locations (black dots) and area in which LKC CO_2 storage estimates were calculated (stippled, square mile). LKC_A–LKC_F = zones within the Pennsylvania Lansing and Kansas City groups; msl = mean sea level; SHRU 86A = Sleepy Hollow Reagan unit 86A.

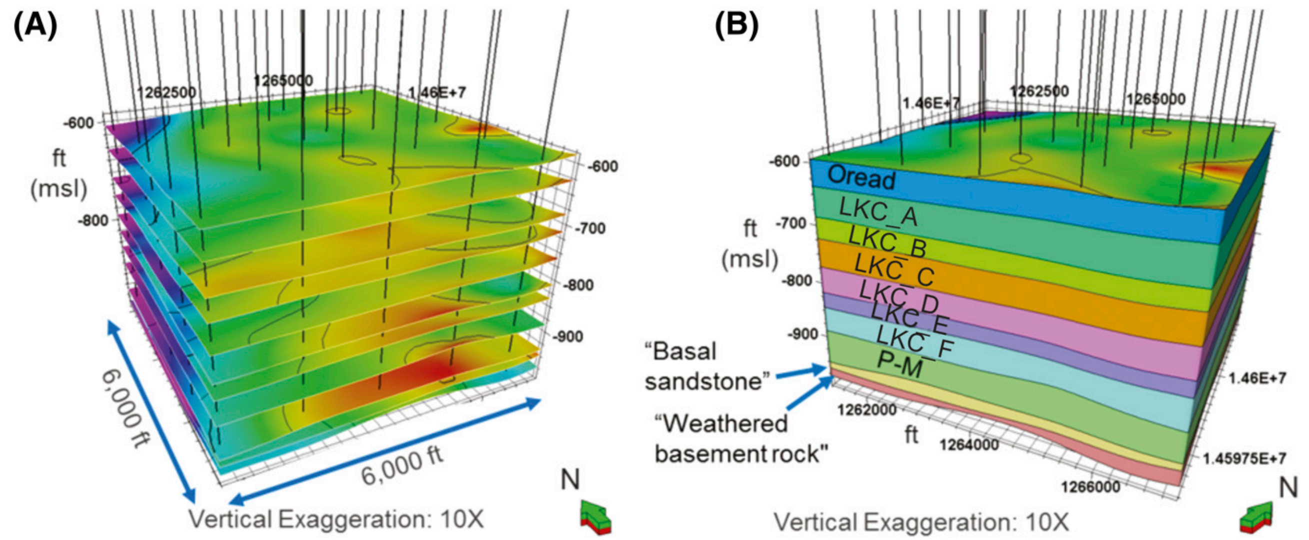

Figure 10. The static earth (SE) model surfaces and framework. (A) Surfaces representing the tops of key carbonate rock units; vertical black lines are wells. (B) The SE model with zones defined by surfaces. The SE model framework is 6000 × 6000 × 384 ft thick (1828 × 1829 × 117 m) and referenced to mean sea level (msl). LKC = Pennsylvanian Lansing and Kansas City groups; P-M = undifferentiated Pleasanton and Marmaton groups.

generate values no smaller or larger than the minimum and maximum values of the input data, respectively. The moving average interpolation technique finds an average of the input data and weighs according to the distance from the wells. The horizontal setting was isotropic, and the vertical range was set to 2 ft (0.61 m) (Figure 12). The moving average method was selected because the correlation of GR logs showed that facies could usually be traced across the entire oil field. This facies model is continuous, and a discrete version of it is derived through the GR thresholds as described previously and summarized in Table 3.

Porosity Model

Effective porosity logs were derived from NPHI logs, and they were corrected using the V-shale approach as explained previously. A salient problem with this approach is that the selection of an appropriate maximum GR value can be difficult, especially when certain transgressive marine shales (core shales of Heckel, 1986, 1994, 2008) produce large GR values. The resulting effective porosity logs for mudstone intervals were considered too large, with many values above 10% (Figure 13A). To remediate this problem, effective porosity logs were attenuated (with an attenuation multiplier of $((150–GR)/150)^2$) such that the effective porosity of the mudstone intervals would be equal to or less than the effective porosities of regressive limestones (Figure 13B). For clean (i.e., relatively clay-free) limestones as validated with ECS response (Figure 11A), NPHI was considered to be a reliable estimate of effective porosity; therefore, raw NPHI log values for these strata were used without any adjustments.

Following the adjustments to the effective porosity logs, the 3-D effective porosity model was prepared in three steps: (1) The effective porosity logs at 0.5-ft intervals were upscaled (sampled) into the model's 2-ft layer grid along the well trajectories using an arithmetic mean method. Basically, porosity is an additive property and so the mean porosity values were computed over 2-ft intervals using mean = $(n_1+n_2+n_3+n_4)/4$. (2) An experimental variogram was fit to the sampled effective porosity logs and was provided as geostatistical input to the Gaussian random function simulation (GRFS) method. (3) The GRFS method was run using the effective porosity as the primary input and was collocated, cokriged with the GR facies model as secondary input to produce the 3-D effective porosity model (Figure 14). Unlike the kriging method that produces values that tighten toward the population's mean value, the GRFS method was selected because it can produce local variations (heterogeneity) that can fully honor the variance from the input porosity data while supervised by variogram statistics. The disadvantage of this method is that a single GRFS run produces just one equal probable distribution.

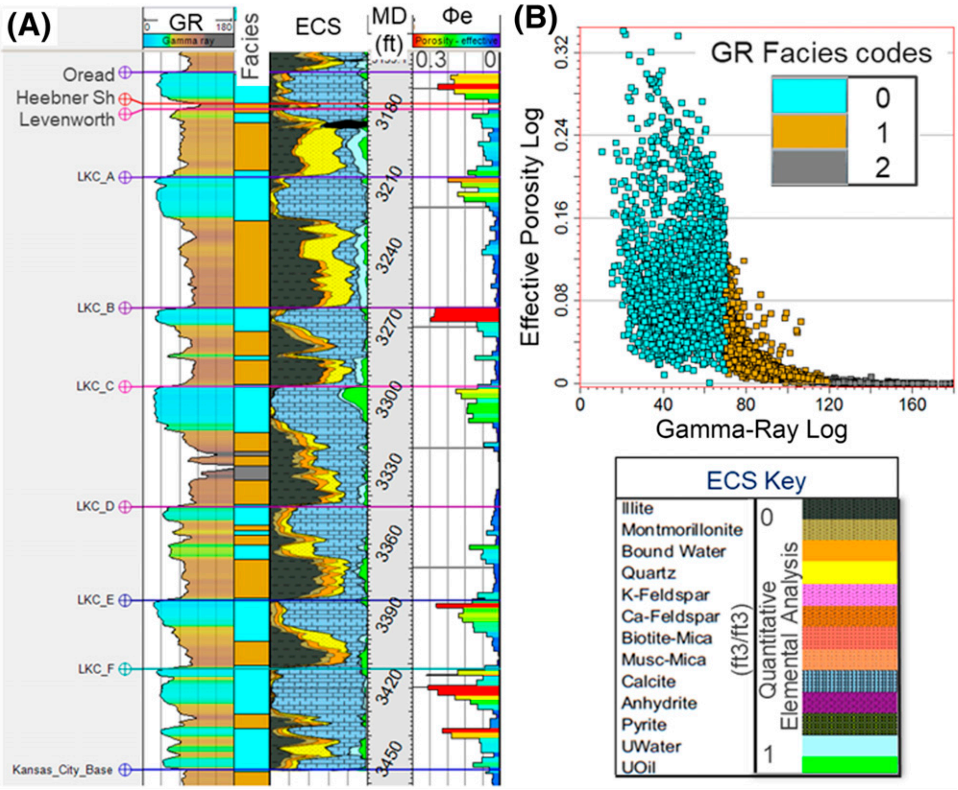

Figure 11. Pennsylvanian Lansing and Kansas City groups (LKC) facies delineation through gamma-ray (GR) log thresholds. (A) The GR log, facies codes, elemental capture spectroscopy (ECS), and effective porosity for the LKC. (B) Effective porosity versus GR showing porosity partitioned by facies. ϕe = effective porosity; LKC_A–LKC_F = zones within the Pennsylvania Lansing and Kansas City groups; MD = measured depth; Musc = muscovite; Sh = Shale; UOil = movable oil; Uwater = movable water.

Permeability Model

Based on existing laboratory measured core data, the permeability logs were derived from a power-law regression between core porosity and core permeability ($K = 180.73* \psi_e$^1.91). This regression or fit was then used to calculate permeability logs from the effective porosity logs.

The 3-D permeability model was prepared in a three-step process: (1) The permeability logs at 0.5-ft intervals were sampled into the model's 2-ft layer grid along the well trajectories using a harmonic mean method, where the mean = $4/(1/n_1+1/n_2+1/n_3+1/n_4)$. The harmonic mean upscaling method produces more representative estimates of permeability across vertical layers (Fouda, 2016). (2) The GRFS method was run using the sampled permeability logs as the primary input and was collocated, cokriged with the effective porosity model as secondary input to produce the 3-D permeability model (Figure 15). This approach produced a 3-D permeability model that spatially correlates to the effective porosity model.

Storage Capacity Estimates

For temperatures greater than 31.1°C and pressures greater than 7.38 MPa (>1070.4 psi), the critical point, CO_2 is in a supercritical state. Drill-stem testing in the Wabaunsee Group, Oread, and the lower Marmaton Group produced data that were used to determine the reservoir temperature and pressure gradients. These gradients were then used to prepare temperature and pressure models within the 3-D grid. The grid was then populated with a CO_2 density model using a pressure-temperature lookup table. With increasing depth, the top and base of the LKC had the following ranges of reservoir conditions and CO_2 density.

Temperature: 34.3°C–36.3°C
Pressure: 1545–1730 psi (10.65–11.93 MPa)
Density: 743–753 kg/m^3 (46.38–47.00 lb/ft^3).

The common method for calculating CO_2 storage potential in saline formations is given by the following equation from Peck et al. (2014):

Table 3. Gamma-Ray Facies Codes Used in This Study

Gamma-Ray Facies Code and (Gamma-Ray Log)	Lithology	Depositional Setting	Porosity and Permeability
0 (0–70 gAPI)	Carbonate-dominated; oolitic, peloidal, and skeletal grainstones are of special interest as reservoir rocks. Also includes other carbonate rock types, including mudstones and wackestones.	Transgressive or regressive offshore marine. Porosity may be enhanced through subaerial exposure and infiltration by meteoric water.	Good porosity development. Regressive packages tend to be thicker than transgressive ones. In the absence of an intervening unit of gamma-ray facies 2, successive regressive and transgressive packages may appear as a single, thick carbonate succession 0.1 md $< K <$ 50 md.
1 (70–120 gAPI)	Mudstone-dominated, includes reddish siliciclastic mudstones, with pedogenetic features.	Regressive, nearshore-marine depositional environment subjected to subaerial exposure, oxidation, and soil development during and after regression.	Considered tight. Has high total porosity because of water-bound clay. Effective porosity likely poor. Core reports commonly show permeability as 0.001 md.
2 (120+ gAPI)	Black or dark gray shale. At SHF, usually absent.	Transgressive marine.	Tight. For modeling purposes, this shale is grouped with gamma-ray facies code 1. Core permeability at 0.001 md.

Abbreviations: K = permeability; SHF = Sleepy Hollow field.

$$M_{CO_2} = A \times h \times \phi_t \times \rho_{CO_2} \times E_{saline} \quad (3)$$

where

M_{CO_2} = mass estimate of CO_2 storage resource;
A = total area;
h = gross formation thickness;
ϕ_t = total porosity;
ρ_{CO_2} = CO_2 density at in situ pressure and temperature; and
E_{saline} = fraction of the total reservoir pore volume that is filled by CO_2; E_{saline} is a scalar value less than 1 and represents the fraction of the pore space that is accessible.

Equation 3 was adapted for use in a 3-D geocellular model such that estimates of CO_2 storage mass can be computed directly on individual cells and added together to produce CO_2 storage mass estimates (Equation 4). Furthermore, because we use effective porosity rather than total porosity and use GR facies to identify the reservoir rock, the storage efficiency factor is simplified to just the displacement terms: $E_{saline} = (E_v \times E_d)$ where E_v is the volumetric displacement efficiency factor and E_d is the microscopic displacement efficiency factor. We used $E_{saline} = 0.1$ to represent the 10 percent probability (p10) level for limestone per Peck et al. (2014) because the area and thickness of the reservoir rock was well defined. Thus, M_{CO_2} could be computed and reported by the LKC zone and by GR facies:

$$M_{CO_2} = Vc \times \phi_e \times \rho_{CO_2}(P, T) \times E_{saline} \quad (4)$$

where

Vc = cell bulk volume;
ϕ_e = cell effective porosity;
$\rho_{CO_2}(P,T)$ = cell CO_2 density based on cell pressure (P) and cell temperature (T); and
E_{saline} = saline storage efficiency factor based on cell GR facies code. For limestone reservoir rock, 0.1 was used.

Finally, the CO_2 storage resource estimate for the LKC was computed using the 3-D SE model, which included bulk volume (Vc), and models for effective porosity (ϕ_e), pressure (P), temperature (T), CO_2 density ($\rho_{CO_2}(P,T)$), and a storage efficiency factor of 0.1. Results are provided in Table 4 based on 1 mi^2 of LKC section at SHF. The calculation assumed that all units were saline and that the formation was accessible

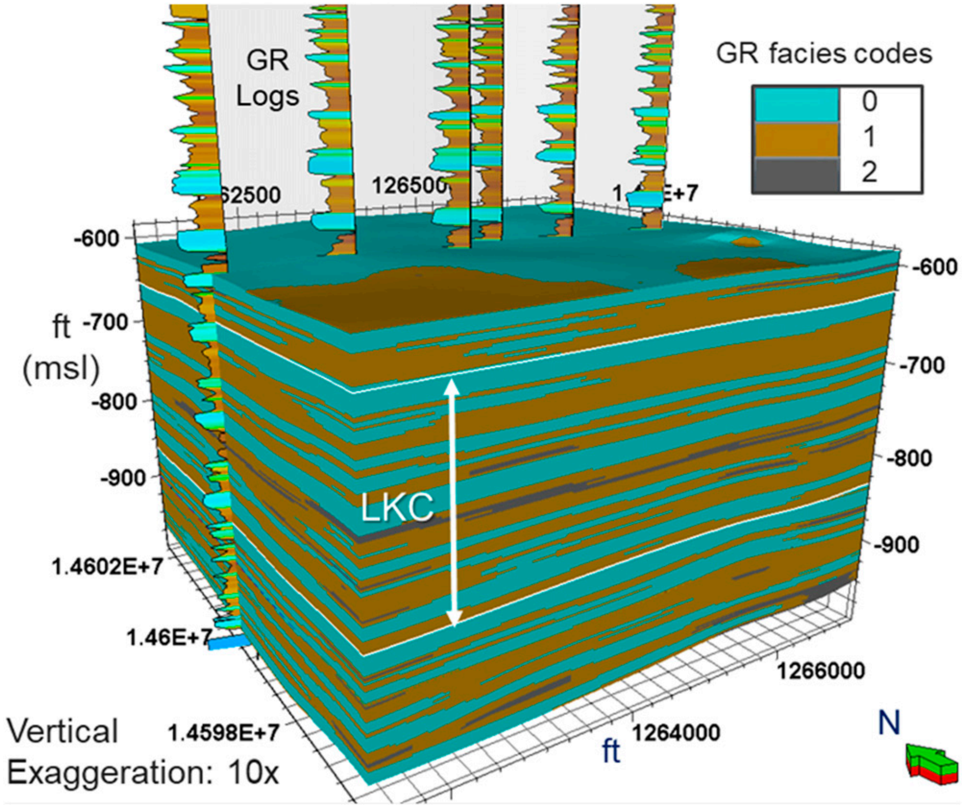

Figure 12. Facies model based on gamma-ray (GR) facies described in Table 3. LKC = Pennsylvanian Lansing and Kansas City groups. msl = mean sea level.

As anticipated, storage of the CO_2 occupies the carbonate units and is partitioned by the mudstone units (Figure 16). Back calculations show that for an LKC carbonate lithology with GR facies code 0, the typical SE model cell ($50 \times 50 \times 2$ ft) or ($15.4 \times 15.4 \times 0.61$ m) holds an average of 870 kg of CO_2 with an average effective porosity of 8.2%.

DISCUSSION

Core examinations and petrography show that the carbonate units vary in composition. The modeling of the carbonate units here used a "lumped" approach because developing a facies model incorporating each lithology (oolite, packstone, wackestone, etc.) would be impractical and difficult to fully validate. Instead, we let the variability of the porosity logs speak for themselves as to the availability of porosity in the carbonate units.

The GR facies code 0 (Table 3) represents the carbonate intervals where regressive limestones are the key porous units in our storage capacity estimates and occur where GR log response is less than 70 gAPI. This criteria targets rock that is potentially accessible to injected CO_2 through interconnected porosity. Within the LKC, GR values greater than 70 are generally mudstone, or if limestone is present, there is significant clay content occluding pore space.

The CO_2 storage estimates presented here were simplified by assuming that all LKC zones were saline. However, Sleepy Hollow is a mature oil field that has produced oil from the LKC zone C and the basal sandstone. Oil shows are also present in LKC zones B and F. A more accurate determination of potential CO_2 storage here would require a more rigorous analysis of water saturation for oil-bearing units.

The deterministic CO_2 mass estimates produced here are comparable to those first produced by Bacon et al. (2018) using National Energy Technology Laboratory carbon dioxide storage prospective resource estimation excel analysis (NETLCO2-SCREEN) (Goodman et al., 2016). The conservative saline efficiency factor of 0.1 reflects limitations to accessible pore volume and represents the combined E_v and E_d.

Accurate calculation of theoretical and practical CO_2 storage capacity in mature oil fields depends

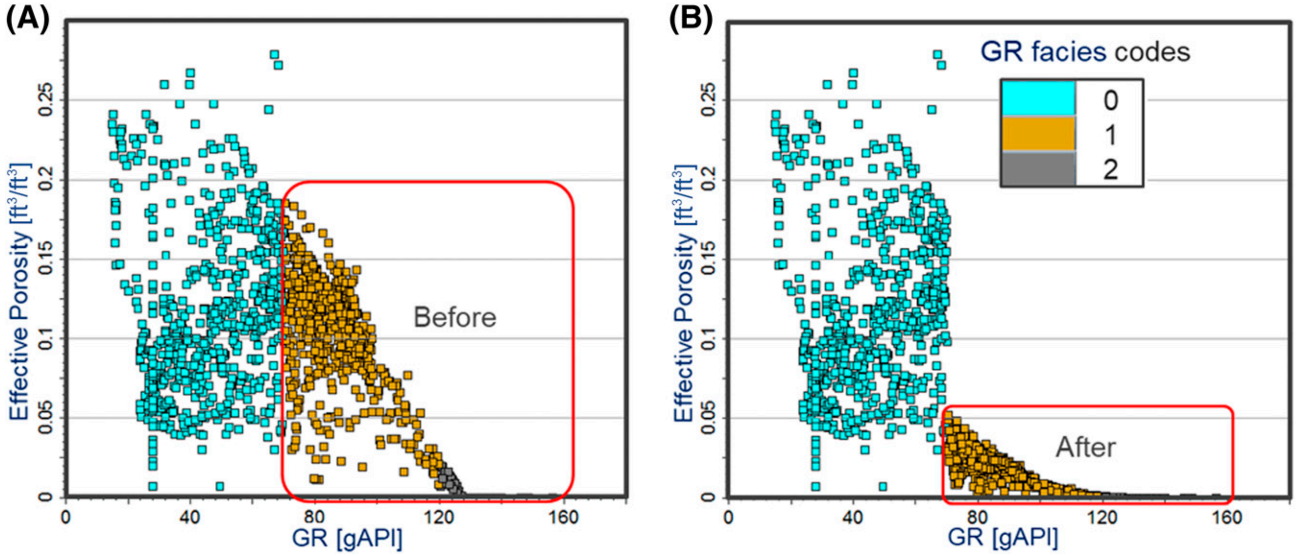

Figure 13. Effective porosity logs for carbonate, mudstone, and shale lithologies. (A) Effective porosity partitioned by facies after shale volume (V-shale) correction. (B) Same data set with further attenuation to effective porosity logs representing mudrocks and shales; thus, red boxes encompass same population of datapoints. For explanation of electrofacies codes (0, 1, 2), see Table 3. GR = gamma ray.

on the accurate porosity and permeability estimation and geostatistical distribution of petrophysical properties. Although permeability is an essential part of static earth modeling, it was not used in the CO_2 estimates presented here because it does not explicitly fit into the equations from Peck et al. (2014) or the NETLCO2-SCREEN method (Goodman et al., 2016). The robust SE model prepared here has a fully integrated workflow and can be used to estimate potential CO_2 storage. Furthermore, this SE model, including the permeability model, can be used as input for dynamic reservoir modeling or flow simulations, which are valuable for estimating storage capacity and injectivity of the formations and for testing different injection strategies.

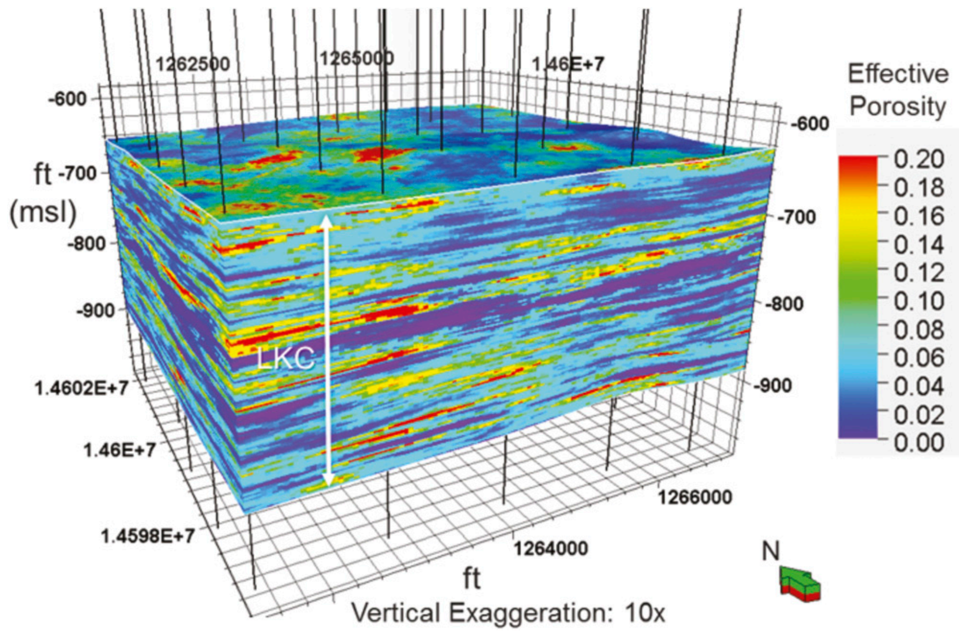

Figure 14. Effective porosity model. Porous Pennsylvanian Lansing and Kansas City groups (LKC) zones correspond to carbonate units. msl = mean sea level.

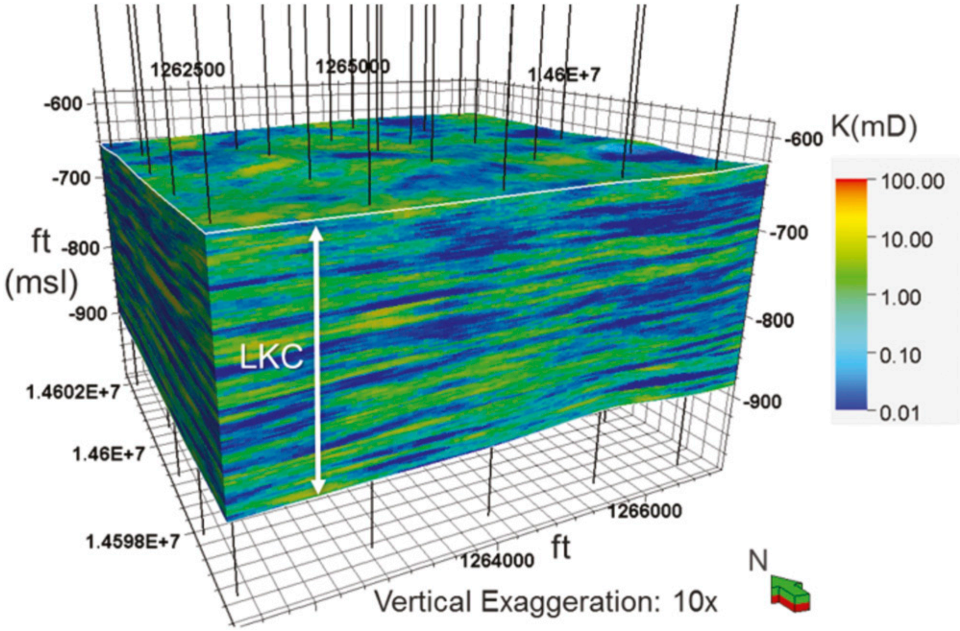

Figure 15. Permeability (K) model. Permeable Pennsylvanian Lansing and Kansas City groups (LKC) zones correspond to limestone units. msl = mean sea level.

SUMMARY AND CONCLUSIONS

Well logs and core data were used to develop an SE model representing the Upper Pennsylvanian LKC at SHF, Nebraska. These data were supplemented with new data from the SHRU 86A drilled expressly for the IMSCS Hub project. A GR facies model representing the limestone, mudstone, and shale units of the LKC was based on GR logs that were widely available. This facies model was used to condition the 3-D effective porosity model that was generated through GRFS and guided by variogram analysis. The CO_2 storage estimates were computed directly from the 3-D geocellular grid containing models for effective volume (of limestone reservoir rock), effective porosity, and CO_2 density (as a function of pressure and temperature). The 1 mi^2 assessment conducted here can serve as a comparative benchmark for CO_2 storage in the LKC. The geologic interpretation and workflows developed in the study provide the basis for commercial CO_2 storage efforts in vertically stacked saline zones along with combined storage through CO_2-EOR in oil-bearing intervals of the Pennsylvanian LKC.

From this study, we make the following conclusions:

1. The CO_2 storage opportunities in the Pennsylvanian LKC are limited to thin (2–22-ft [0.61–6.7-m]-thick) limestone units that are overlain by mudstones. These limestones may be mostly wackestones and mudstones, but oolitic limestone and skeletal and peloidal grainstones are also present and offer the most favorable porosity values. The mudstone units are tight and can act as barriers to upward CO_2 fluid migration. Lateral CO_2 migration within the carbonate units is expected and necessary. Based on project size, flow simulations would be required to develop an injection strategy and delineate CO_2 plume area.

Table 4. Carbon Storage Resource Estimates for the Pennsylvanian Lansing and Kansas City Groups Carbonate Reservoir Units, Gamma-Ray Facies Code 0

LKC Unit	Effective Reservoir, %*	Tonnes CO_2/mi^2	Tonnes CO_2/km^2
LKC zone A	37	89,591	34,591
LKC zone B	40	79,587	30,729
LKC zone C	38	116,636	45,033
LKC zone D	39	74,597	28,802
LKC zone E	54	85,686	33,084
LKC zone F	76	156,060	60,255
Total		602,157	232,494

Abbreviation: LKC = Pennsylvanian Lansing and Kansas City groups.
*Percent of zonal volume comprised of limestone reservoir rock; remaining zonal part is either mudstone or shale.

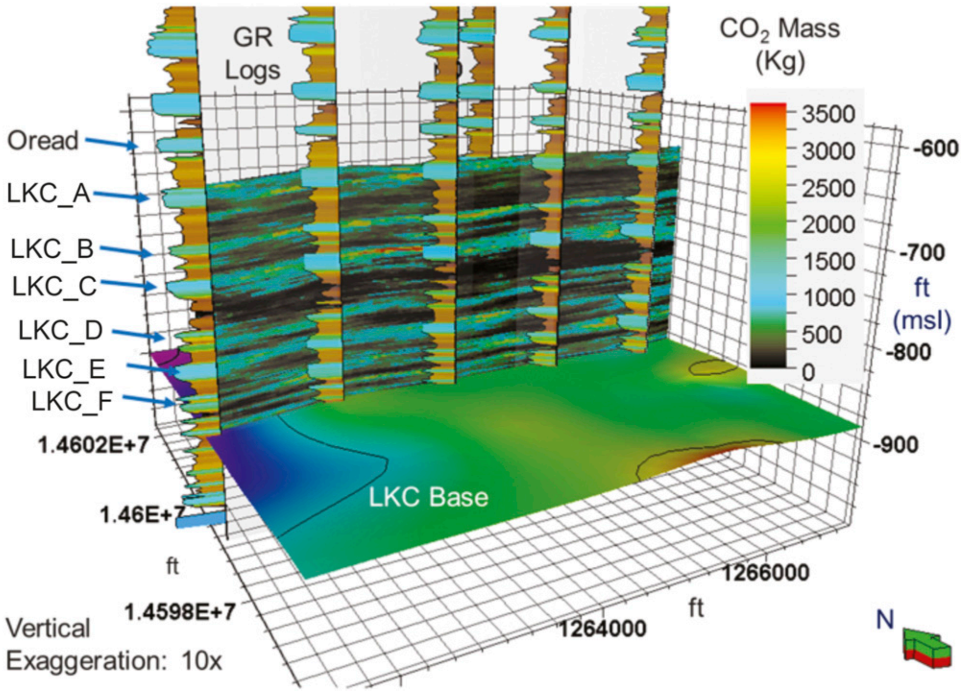

Figure 16. Slice through the static earth model showing the computed CO_2 mass storage for the Pennsylvanian Lansing and Kansas City groups (LKC). Dark areas represent mudstone intervals. Light areas represent computed CO_2 storage based on CO_2 density and reservoir pore space accessibility. GR = gamma ray; LKC_A–LKC_F = zones within the Pennsylvania Lansing and Kansas City groups; msl = mean sea level.

2. The Kansas-type cyclothem model provides a practical basis for understanding the LKC carbonate succession, but the outcrop-based model proposed by previous authors requires revision. For our study area on the Cambridge arch, we have determined that transgressive marine shales are commonly absent or are too thin to be detected with well logs alone.
3. Many wells in the study area have GR logs and their low response to clean carbonates (GR < 70 gAPI) can be used to identify and partition limestone units from the mudrock–dominated intervals. This partitioning in turn can be used to build a GR facies model.
4. The NPHI logs provide good estimates of effective porosity in clean limestone units. In contrast, clay-bound water in mudstone-dominated units require significant corrections to produce an effective porosity for these intervals. Calibrating effective porosity and permeability logs requires laboratory core data. Unfortunately, the high porosity values from the mudstone samples are not considered effective porosity when paired with permeability values of 0.001 md. Alternately, measurements on limestone core have provided the best evidence of porosity and permeability.
5. The GR logs alone cannot be used to identify individual limestone textures.
6. The relative thinness of limestones and their pore-space limitations are crucial restrictions for CO_2 storage in the LKC. Nevertheless, these restrictions do not preclude significant potential for regional storage in and around existing, mature oil fields.
7. At SHF, the supercritical CO_2 storage is estimated at 602,157 t/mi^2 (232,494 t/km^2) when using a deterministic saline storage efficiency factor of 0.1.

Current work involves laboratory measurements on new core samples, but opportunities remain for the refinement of effective porosity logs and the development of accurate permeability logs. Laboratory-based NMR measurements on core samples may provide new data to better calibrate effective porosity logs. A more robust treatment of CO_2 storage estimates in the LKC would require further characterization of oil-bearing intervals. Additionally, a probabilistic treatment of the storage efficiency factors would yield estimated storage results for p10, p50, and p90. This workflow is currently being developed as part of an integrated solution.

REFERENCES CITED

Bacon, D. H., D. Blankenau, D. Divine, A. Duguid, I. Fukai, J. Glier, J. Hawkins, M. Jimenez et al., 2018, Integrated mid-continent stacked carbon storage hub, phase 1 final report: Washington, DC, US Department of Energy, 275 p., accessed April 16, 2020, https://www.osti.gov/biblio/1478726-integrated-mid-continent-stacked-carbon-storage-hub-phase-final-report.

Busch, K., 1977, Structure and stratigraphy of the B zone (Lansing–Kansas City Groups) in Red Willow County, Nebraska, Master's thesis, University of Nebraska at Lincoln, Lincoln, Nebraska, 157 p.

Dubois, M. K., 1985, Application of cores in development of an exploration strategy for the Lansing–Kansas City "E" zone, Hitchcock County, Nebraska: Lawrence, Kansas, Kansas Geological Survey Subsurface Geology Series 6, p. 120–132.

Evans, D. G., and D. W. Steeples, 1987, Microearthquakes near the Sleepy Hollow oil field, southwestern Nebraska: Bulletin of the Seismological Society of America, v. 77, no. 1, p. 132–140.

Fouda, M. A. G., 2016, Relative permeability upscaling for heterogeneous reservoir models, Ph.D. dissertation, Heriot-Watt University, Edinburgh, Scotland, 160 p.

Goodman, A., S. Sanguinito, and J. S. Levine, 2016, Prospective CO_2 saline resource estimation methodology: Refinement of existing US-DOE-NETL methods based on data availability: International Journal of Greenhouse Gas Control, v. 54, p. 242–249, doi:10.1016/j.ijggc.2016.09.009.

Heckel, P. H., 1986, Sea-level curve for Pennsylvania eustatic marine transgressive-regressive depositional cycles along midcontinent outcrop belt, North America: Geology, v. 14, no. 4, p. 330–334, doi:10.1130/0091-7613(1986)14<330:SCFPEM>2.0.CO;2.

Heckel, P. H., 1991, Thin widespread Pennsylvanian black shales of the Midcontinent North America: A record of a cyclic succession of widespread pycnoclines in a fluctuating epeiric sea: Geological Society, London, Special Publications 1991, v. 58, p. 259–273.

Heckel, P. H., 1994, Evaluation of evidence for glacio-eustatic control over marine Pennsylvanian cyclothems in North America and consideration of possible tectonic effects, *in* J. Dennison and F. R. Ettensohn, eds., Concepts in Sedimentology and Paleontology: SEPM 4, p. 65–87.

Heckel, P. H., 2008, Pennsylvanian cyclothems in Midcontinent North America as far-field effects of waxing and waning of Gondwana ice sheets, *in* C. R. Fielding, T. D. Frank, and J. L. Isbell, eds., Resolving the late Paleozoic ice age in time and space: Geological Society of America Special Paper 441, p. 275–289.

Heckel, P. H., and W. L. Watney, 2002, Revision of stratigraphic nomenclature and classification of the Pleasanton, Kansas City, Lansing, and lower part of the Douglas Groups (Lower Upper Pennsylvanian, Missourian) in Kansas: Lawrence, Kansas, Kansas Geological Survey Bulletin 246, 75 p.

Joeckel, R. M., 1989, Geomorphology of a Pennsylvanian land surface: Pedogenesis in the Rock Lake Shale Member, southeastern Nebraska: Journal of Sedimentary Petrology, v. 59, p. 469–481, doi:10.1306/212F8FC6-2B24-11D7-8648000102C1865D.

Joeckel, R. M., 1994, Virgilian (Upper Pennsylvanian) Paleosols in the upper Lawrence Formation (Douglas Group) and its Snyderville Shale Member (Oread Formation, Shawnee Group) of the Northern Midcontinent, U.S.A.: Pedologic contrasts in a cyclothem sequence: Journal of Sedimentary Research, v. 64, no. 4a, p. 853–866, doi:10.1306/D4267EE7-2B26-11D7-8648000102C1865D.

Joeckel, R. M., 1999, Paleosol in Galesburg Formation (Kansas City Group, Upper Pennsylvanian), northern Midcontinent, U.S.A.: Evidence for climate change and mechanisms of marine transgression: Journal of Sedimentary Research, v. 69, no. 3, p. 720–737, doi:10.2110/jsr.69.720.

Moore, V. A., and R. B. Nelson, 1974, Effect of Cambridge-Chadron structural trend on Paleozoic and Mesozoic thickness, western Nebraska: AAPG Bulletin, v. 58, no. 2, p. 260–268.

Peck, W. A., K. A. Glazewski, R. C. L. Klenner, C. D. Gorecki, E. N. Steadman, and J. A. Harju, 2014, A workflow to determine CO_2 storage potential in deep saline formations: Energy Procedia, v. 63, p. 5231–5238, doi:10.1016/j.egypro.2014.11.554.

Prather, B. E., 1985, Depositional facies and diagenetic fabrics of the D-zone cyclothem, Lansing-Kansas City groups, Hitchcock County, Nebraska: Lawrence, Kansas, Kansas Geological Survey Subsurface Geology 6, p. 133–144.

Rogers, J. P., 1977, Genesis and distribution of Desmoinesian (Pennsylvanian) Sandstone Reservoir, Sleepy Hollow Field, Red Willow County, Nebraska: AAPG Bulletin, v. 61, no. 7, p. 1029–1044.

Watney, W. L., 1980, Cyclic sedimentation of the Lansing-Kansas City Groups in northwestern Kansas and southwestern Nebraska: Lawrence, Kansas, Kansas Geological Survey Bulletin 220, 80 p.

Young, A. L., 2011, Lithostratigraphy and diagenesis of the Upper Pennsylvanian (Missourian) Lansing-Kansas City Groups in Rooks County, Kansas, Master's thesis, Wichita State University, Wichita, Kansas, 30 p.